Type 1 Diabetic Akita Mouse Hearts Are Insulin Sensitive but Manifest Structurally Abnormal Mitochondria That Remain Coupled Despite Increased Uncoupling Protein 3

Heiko Bugger,[1] Sihem Boudina,[1] Xiao Xuan Hu,[1] Joseph Tuinei,[1] Vlad G. Zaha,[1]
Heather A. Theobald,[1] Ui Jeong Yun,[1] Alfred P. McQueen,[2] Benjamin Wayment,[2] Sheldon E. Litwin,[2]
and E. Dale Abel[1]

OBJECTIVE—Fatty acid–induced mitochondrial uncoupling and oxidative stress have been proposed to reduce cardiac efficiency and contribute to cardiac dysfunction in type 2 diabetes. We hypothesized that mitochondrial uncoupling may also contribute to reduced cardiac efficiency and contractile dysfunction in the type 1 diabetic Akita mouse model (Akita).

RESEARCH DESIGN AND METHODS—Cardiac function and substrate utilization were determined in isolated working hearts and in vivo function by echocardiography. Mitochondrial function and coupling were determined in saponin-permeabilized fibers, and proton leak kinetics was determined in isolated mitochondria. Hydrogen peroxide production and aconitase activity were measured in isolated mitochondria, and total reactive oxygen species (ROS) were measured in heart homogenates.

RESULTS—Resting cardiac function was normal in Akita mice, and myocardial insulin sensitivity was preserved. Although Akita hearts oxidized more fatty acids, myocardial O_2 consumption was not increased, and cardiac efficiency was not reduced. ADP-stimulated mitochondrial oxygen consumption and ATP synthesis were decreased, and mitochondria showed grossly abnormal morphology in Akita. There was no evidence of oxidative stress, and despite a twofold increase in uncoupling protein 3 (UCP3) content, ATP-to-O ratios and proton leak kinetics were unchanged, even after perfusion of Akita hearts with 1 mmol/l palmitate.

CONCLUSIONS—Insulin-deficient Akita hearts do not exhibit fatty acid–induced mitochondrial uncoupling, indicating important differences in the basis for mitochondrial dysfunction between insulin-responsive type 1 versus insulin-resistant type 2 diabetic hearts. Increased UCP3 levels do not automatically increase mitochondrial uncoupling in the heart, which supports the hypothesis that fatty acid–induced mitochondrial uncoupling as exists in type 2 diabetic hearts requires a concomitant increase in ROS generation. *Diabetes* **57:2924–2932, 2008**

Cardiac efficiency is the ratio of cardiac work to myocardial O_2 consumption (Vo_2). Impaired cardiac efficiency has been proposed to be an underlying mechanism leading to cardiac contractile dysfunction in type 2 diabetes (1,2). In type 2 diabetic *db/db* and *ob/ob* mice, increased fatty acid utilization and myocardial Vo_2 are not accompanied by a proportionate increase in contractile function, resulting in reduced cardiac efficiency (3,4). We previously demonstrated that fatty acid–induced mitochondrial uncoupling occurs in the hearts of these mice and likely results from activation of cardiac uncoupling proteins (5,6). Thus, increased fatty acid utilization in type 2 diabetic hearts is associated with mitochondrial uncoupling, which leads to decreased ATP production. This prevents a proportionate increase in cardiac work and results in reduced cardiac efficiency (1). The presence of increased mitochondrial reactive oxygen species (ROS) production in *db/db* mice and the ability of ROS to activate uncoupling proteins also suggested that fatty acid–induced mitochondrial uncoupling in these hearts required the presence of increased ROS (6,7). Although fatty acid–induced uncoupling may contribute to reduced cardiac efficiency in type 2 diabetic models, it is not known whether mitochondrial uncoupling also contributes to impaired cardiac efficiency and contractile dysfunction in models of type 1 diabetes.

Most studies of type 1 diabetes in rodents have been performed after induction of diabetes with streptozotocin. In streptozotocin-induced diabetic mice, many cardiac alterations are similar to type 2 diabetic hearts, such as increased fatty acid oxidation, reduced glucose oxidation, impaired mitochondrial respiration, oxidative stress, and impaired contractile function (8–11). In addition, it was reported that cardiac efficiency was reduced in streptozotocin-injected animals, and expression of uncoupling protein 3 (UCP3) was increased (8,12). These similarities to type 2 diabetic models prompted us to investigate in this study whether mitochondrial uncoupling also contributes to impaired cardiac efficiency and contractile dysfunction in type 1 diabetic models. To date, measurements of cardiac state 4 respiration rates and ADP-to-O ratios performed in streptozotocin-injected animals have yielded conflicting results, making it difficult to make any conclusions about the presence or absence of mitochondrial uncoupling in this model of type 1 diabetes (8,13–15).

Potential extrapancreatic toxic effects are a disadvantage of the streptozotocin model, in particular when high-dose streptozotocin administration is used (16). In

addition, the severity of diabetes can vary considerably in this model, and mitochondrial dysfunction may or may not occur (17). To circumvent these concerns, genetic models of type 1 diabetes are increasingly used, and the Animal Models of Diabetic Complications Consortium (AMDCC) has proposed the Akita diabetic mouse as a useful model with which to study the chronic complications of type 1 diabetes (18). This mouse develops diabetes as a consequence of a single base pair substitution in the *Ins2* gene, resulting in improper folding of proinsulin, which leads to protein aggregate–induced endoplasmic reticulum stress in pancreatic islets (19,20) and eventual β-cell failure (19). Akita mice are severely hyperglycemic by 5–6 weeks of age and develop typical chronic complications of diabetes, such as retinopathy, neuropathy, and nephropathy (21,22).

In this study, we hypothesized that mitochondrial uncoupling may also contribute to reduced cardiac efficiency and contractile dysfunction in type 1 diabetes. To test our hypothesis, we measured cardiac contractile function, energy substrate metabolism, and mitochondrial function and coupling in the type 1 diabetic Akita mouse model (Akita). The main finding of this study was that Akita hearts are protected from fatty acid–induced mitochondrial uncoupling despite increased UCP3 expression. Our data imply that mechanisms for mitochondrial dysfunction differ importantly between insulin-deficient type 1 and insulin-resistant type 2 diabetic hearts.

RESEARCH DESIGN AND METHODS

Male Akita mice (C57BL/6) and C57BL/6 controls were obtained from The Jackson Laboratories (Bar Harbor, ME) and housed at 22°C with free access to water and food with a light cycle of 12 h light and 12 h dark. Animals were studied in accordance with protocols approved by the Institutional Animal Care and Use Committee of the University of Utah. All studies were performed in random-fed animals.

Serum analyses. Free fatty acid concentrations, triacylglycerol levels, and blood glucose levels were measured as previously described (4).

Echocardiography. Contractile function and left ventricular chamber dimensions were measured as described previously (23).

Heart perfusions. Contractile function and substrate metabolism were measured in isolated working hearts perfused with Krebs-Henseleit buffer (KHB) containing 5 mmol/l glucose and 0.4 mmol/l palmitate in the presence or absence of 1 nmol/l insulin as previously described (3). For some mitochondrial respiration studies, hearts were perfused in the Langendorff mode with KHB containing 11 mmol/l glucose and 1 mmol/l palmitate for 30 min (5). The effect of a calcium-induced increase in workload on contractility was investigated in Langendorff-perfused hearts with KHB (5 mmol/l glucose and 0.4 mmol/l palmitate) (5). Hearts were perfused for 40 min, and calcium was raised from 2 to 4 mmol/l after 20 min.

Mitochondrial function. Saponin-permeabilized fibers were prepared from freshly excised or Langendorff-preperfused hearts as described previously (5). Respiration and ATP synthesis were measured using 20 μmol/l palmitoyl carnitine, 10 mmol/l pyruvate, or 5 mmol/l glutamate as substrates, each combined with 2 mmol/l malate. Respiration was measured in the presence of substrate alone (V_0), after addition of 1 mmol/l ADP (V_{ADP}), and after addition of 1 μg/ml F_0F_1-ATPase inhibitor oligomycin (V_{Oligo}).

Proton leak kinetics. Proton leak measurements were performed in hearts that were preperfused for 20 min with 11 mmol/l glucose and 1 mmol/l palmitate. Mitochondria were prepared from whole hearts by differential centrifugation, and proton leak kinetics was measured in the presence of 20 μmol/l palmitoyl carnitine as previously described (6,24).

Electron microscopy. Hearts were freshly excised and immediately washed in ice-cold saline. Samples were collected from left ventricular myocardium and processed as described previously (6). Mitochondrial volume density and number were analyzed by stereology in a blinded fashion using the point-counting method (6,25).

Hydrogen peroxide production. Mitochondrial hydrogen peroxide (H_2O_2) generation was measured using succinate as a substrate as described previously (6). To block H_2O_2 production at complex I, 10 μmol/l rotenone was added to the reaction. Mitochondrial H_2O_2 production is widely accepted as a measure of mitochondrial superoxide production.

Oxidative stress. Tissue ROS levels were measured by the conversion of nonfluorescent 2′, 7′-dichlorofluorescein-diacetate (DCFDA) to the highly fluorescent 2′, 7′-dichlorofluorescein (DCF) in the presence of esterases and ROS (26) (for details, see the supplementary methods available in an online appendix at http://dx.doi.org/10.2337/db08-0079). Activity of mitochondrial aconitase was measured in isolated mitochondria as described previously (27).

RNA extraction and quantitative RT-PCR. Total RNA was extracted from hearts with Trizol reagent (Invitrogen, Carlsbad, CA), purified with the RNEasy kit (Qiagen, Valencia, CA), and reverse transcribed (6). Data were normalized by expressing them relative to the levels of the invariant transcript 16S RNA. Primer sequences and accession numbers are presented in supplementary Table 1.

Western blot analysis. Isolated mitochondria or whole-cell extracts were prepared as described previously and resolved by SDS-PAGE (5,6). For antibody conditions see supplementary methods in the online appendix. Protein concentrations were determined using the Micro BCA Protein Assay kit (Pierce, Rockford, IL), and equal protein loading was verified by Coomassie staining.

Statistical analysis. Data are presented as means ± SE. When comparing two groups, significance was determined using a Student's *t* test. Effects of calcium-induced increase in contractility were analyzed using a paired *t* test. Analysis of working heart perfusions ± insulin was performed using one-way ANOVA. Significance was assessed by Fisher's protected least significant difference test. For all analyses, the Statview 5.0.1 software package was used (SAS Institute, Cary, NC), and significant difference was accepted when $P < 0.05$.

RESULTS

Serum metabolites and cardiac growth. Akita diabetic mice develop type 1 diabetes as early as 5–6 weeks of age and show normal survival until 6 months of age but then show a dramatic decrease in survival with almost no survivors by 12 months of age (19). To investigate the long-term effects of type 1 diabetes on the heart, we chose to investigate mice mainly at 24 weeks of age. Serum glucose levels were markedly increased in Akita mice at 24 weeks of age (138 ± 5 vs. 566 ± 21 mg/dl; $P < 0.05$). Hyperglycemia was accompanied by increased serum fatty acid levels (261 ± 43 vs. 537 ± 72 μmol/l; $P < 0.05$) and increased serum triacylglycerol levels (0.98 ± 0.11 vs. 2.40 ± 0.54 mmol/l; $P < 0.05$). In contrast to wild-type mice, Akita mice showed no increase in body weights as they aged (supplementary Table 2). Heart weights and tibia lengths were measured at 10, 24, and 54 weeks of age in the Akita mice (supplementary Table 2). Although heart-to-tibia length ratios were not different at 10 weeks, we observed reduced ratios at 24 and 54 weeks of age. Heart weight–to–body weight ratios were not reduced, indicating that the reduction in heart size parallels the general catabolic state of diabetic Akita mice.

Cardiac function. Cardiac contractile function and chamber dimensions were examined in Akita diabetic mice by echocardiography at 20, 36, and 54 weeks of age. Fractional shortening and ejection fraction were not different at any age (Table 1), and there were no differences in chamber dimensions in diabetic and nondiabetic mice (supplementary Table 3). Cardiac output was increased at 20 weeks of age but was lower at 54 weeks of age in Akita mice, which was likely due to a moderate but nonsignificant reduction in heart rate. Because adaptations of the neurohumoral system can mask the presence of contractile dysfunction in vivo, we investigated contractile function in isolated working hearts in the absence and presence of insulin (Fig. 1*A*–*C*). In the absence of insulin, left ventricular developed pressure was reduced in 24-week-old Akita mice, and a trend toward increased cardiac output in Akita hearts led to no differences in cardiac power. Insulin had a positive inotropic effect in wild-type

TABLE 1
Echocardiographic evaluation of contractile function in wild-type and Akita mice at 20, 36, and 54 weeks of age

	n	Fractional shortening (%)	Ejection fraction (%)	Heart rate (bpm)	Stroke volume (μl/g body wt)	Cardiac output (μl $\cdot$ min^{-1} $\cdot$ g^{-1} body wt)
Wild type (20 weeks)	9	38.6 ± 2.4	76 ± 3	415 ± 12	1.13 ± 0.03	467 ± 14
Akita (20 weeks)	7	38.7 ± 2.4	76 ± 3	472 ± 31	1.12 ± 0.07	527 ± 15*
Wild type (36 weeks)	6	39.6 ± 1.2	78 ± 1	470 ± 41	0.97 ± 0.04	456 ± 25
Akita (36 weeks)	5	39.7 ± 2.7	78 ± 3	421 ± 29	1.13 ± 0.04*	476 ± 33
Wild type (54 weeks)	6	24.6 ± 1.9	57 ± 3	523 ± 29	1.00 ± 0.10	524 ± 28
Akita (54 weeks)	6	27.6 ± 1.9	62 ± 3	448 ± 28	0.95 ± 0.04	426 ± 28*

Data are means ± SE unless otherwise indicated. *$P < 0.05$ vs. wild type.

hearts, which was blunted in Akita mice. Heart rates (bpm) were not significantly changed from baseline by insulin (basal vs. insulin: wild type, 263 ± 8 vs. 281 ± 8; Akita, 290 ± 5 vs. 310 ± 9). To further evaluate myocardial contractile reserve, Langendorff-perfused hearts were examined under normal and increased calcium concentrations. Contractile parameters were similar in 15-week-old wild-type and Akita mice under baseline conditions (2 mmol/l calcium). Changing perfusion conditions to 4 mmol/l calcium significantly increased systolic pressure, developed pressure, and rate pressure product in wild-type and Akita mice by equivalent extents (supplementary Table 4). Thus, despite persistent hyperglycemia, Akita mice exhibited modest left ventricular dysfunction that was evident mainly in insulin-perfused working hearts. In contrast to *ob/ob* mice (5), short-term inotropic reserves were maintained.

Substrate metabolism, insulin signaling, and cardiac efficiency. Decreased cardiac efficiency is believed to be an important contributor to the development of contractile dysfunction in type 2 diabetic models and has been postulated to result from fatty acid–induced mitochondrial uncoupling (1). We therefore measured cardiac substrate utilization and oxygen consumption in isolated working hearts of 24-week-old Akita mice in the absence and presence of insulin. Palmitate oxidation rates were increased and glucose oxidation rates were decreased in the presence or absence of 1 nmol/l insulin in Akita hearts compared with the wild type (Fig. 1D and E). Despite increased fatty acid oxidation, myocardial Vo_2 and cardiac efficiency were not different between wild-type and Akita mice (Fig. 1G and H). Of interest, metabolic insulin responsiveness was retained in Akita hearts. Thus, insulin-suppressed palmitate oxidation increased glycolysis and glucose oxidation in both wild-type and Akita mice (Fig. 1D–F). Consistent with intact metabolic insulin signaling, insulin-stimulated Akt phosphorylation on Ser[473] was maintained in hearts of 10- and 24-week-old mice (Fig. 2A and B). Thus, despite increased fatty acid utilization, Akita hearts maintained normal insulin sensitivity.

Mitochondrial oxygen consumption and respiratory coupling. The absence of reduced cardiac efficiency was unexpected and revealed an important difference between
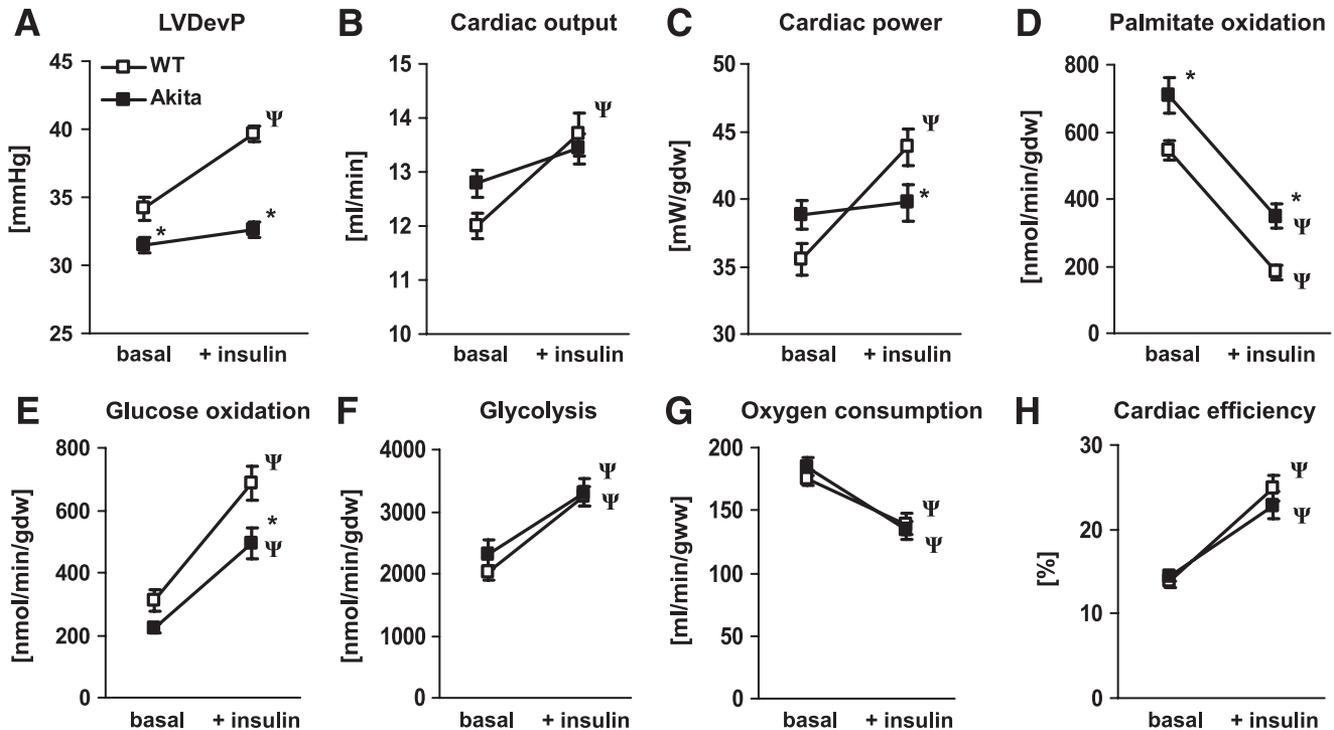

FIG. 1. Substrate oxidation and contractile performance of Akita hearts. 24-week-old wild-type and Akita mouse hearts were perfused in the isolated working mode without insulin (basal) or in the presence of 1 nmol/l insulin ($n = 4$–5). *A*: Left ventricular–developed pressure (LVDevP). *B*: Cardiac output. *C*: Cardiac power. *D*: Palmitate oxidation. *E*: Glucose oxidation. *F*: Glycolysis. *G*: Oxygen consumption. *H*: Cardiac efficiency. *$P < 0.05$ vs. wild type, Ψ$P < 0.05$ vs. without insulin.
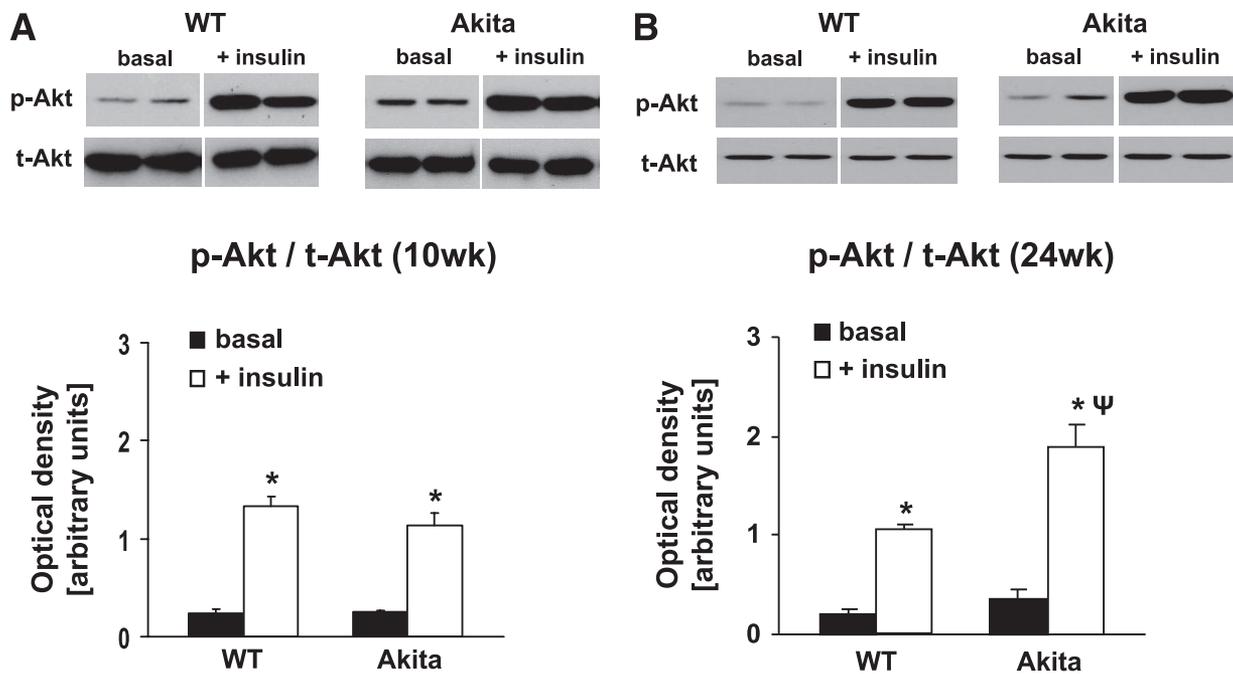
FIG. 2. Intact insulin signaling in Akita hearts. Representative Western blot images showing cardiac protein levels of phosphorylated Akt (p-Akt) on Ser[473] and total levels of Akt (t-Akt) and densitometric quantification of the ratio of p-Akt to t-Akt (p-Akt/t-Akt) after isolated working heart perfusions in the absence (basal) or presence of 1 nmol/l insulin at the age of 10 weeks (*A*) and 24 weeks (*B*). *$P < 0.05$ vs. basal, $\Psi P < 0.05$ vs. wild-type (WT).

the type 1 diabetic Akita mouse and type 2 diabetic mouse models. Because mitochondrial uncoupling may underlie impaired cardiac efficiency in type 2 diabetic hearts (1,5,6), we hypothesized that mitochondrial coupling would be normal in Akita hearts. Mitochondrial function was initially evaluated in fibers that were prepared from freshly isolated mouse hearts. In hearts from 24-week-old mice, maximal ADP-stimulated mitochondrial oxygen consumption (V_{ADP}) and ATP synthesis were unchanged using

palmitoyl carnitine as a substrate (Fig. 3*A* and *E*), but V_{ADP} and ATP synthesis were significantly reduced in Akita mice using pyruvate (Fig. 3*B* and *F*) or glutamate (Fig. 3*C* and *G*) as substrates. Although a respiratory defect was evident, there was no evidence for mitochondrial uncoupling. Rates of oligomycin-insensitive respirations (V_{oligo}) and ATP-to-O ratios were unchanged with any substrate, indicating intact coupling of ATP synthesis to oxygen consumption. In 10-week-old mice, similar reductions in
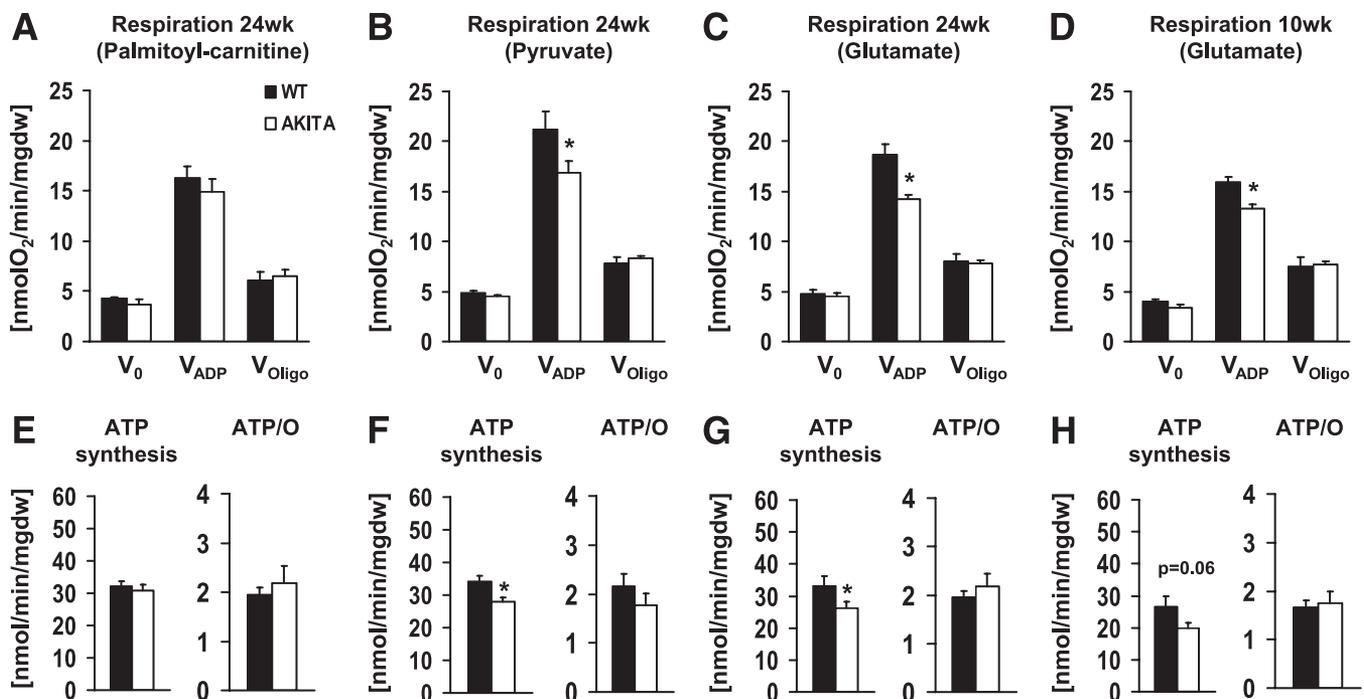

FIG. 3. Preserved mitochondrial coupling and impaired mitochondrial oxidative capacity in Akita hearts. Mitochondrial respiratory rates (*A–C*) and ATP synthesis and ATP-to-O ratios (*E–G*) of saponin-permeabilized cardiac fibers from 24-week-old wild-type (WT) and Akita mice using palmitoyl carnitine (*A* and *E*), pyruvate (*B* and *F*), or glutamate (*C* and *G*) as a substrate (*n* = 6). Similar data were also obtained in 10-week-old mice after incubation with glutamate (*D* and *H*), *n* = 6. *$P < 0.05$ vs. wild type.
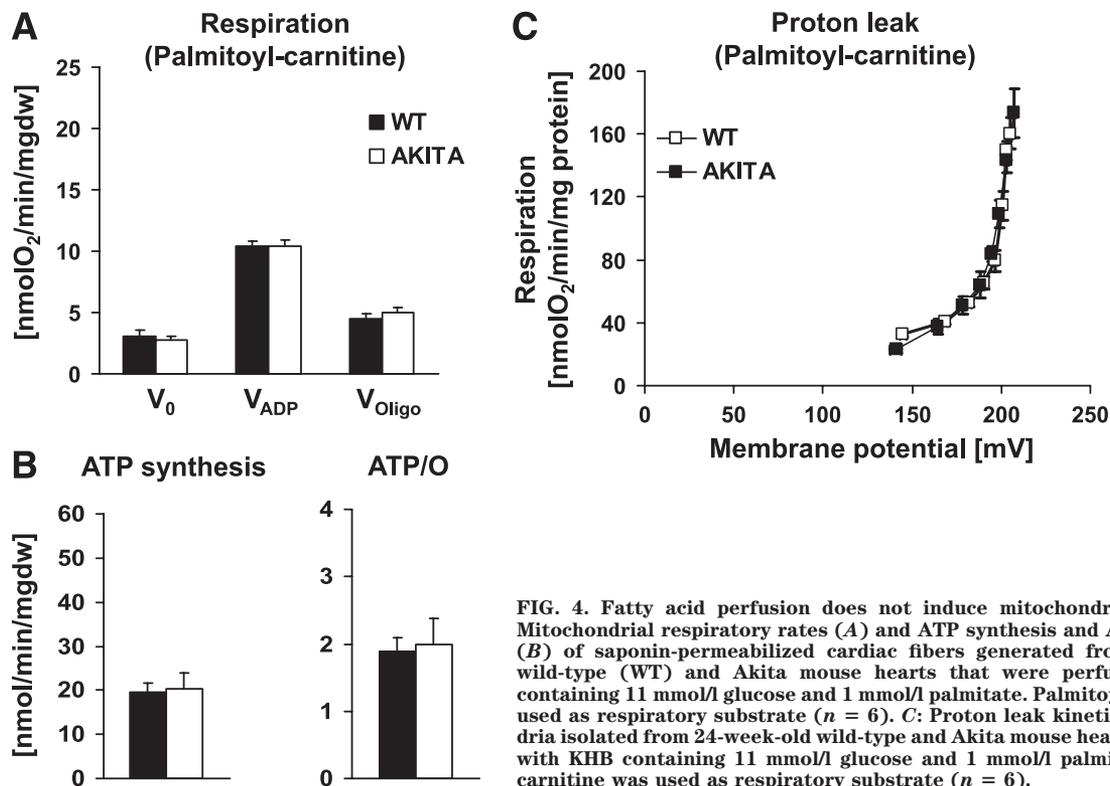
FIG. 4. Fatty acid perfusion does not induce mitochondrial uncoupling. Mitochondrial respiratory rates (A) and ATP synthesis and ATP-to-O ratios (B) of saponin-permeabilized cardiac fibers generated from 24-week-old wild-type (WT) and Akita mouse hearts that were perfused with KHB containing 11 mmol/l glucose and 1 mmol/l palmitate. Palmitoyl carnitine was used as respiratory substrate ($n = 6$). C: Proton leak kinetics of mitochondria isolated from 24-week-old wild-type and Akita mouse hearts preperfused with KHB containing 11 mmol/l glucose and 1 mmol/l palmitate. Palmitoyl carnitine was used as respiratory substrate ($n = 6$).

glutamate-supported respirations (V_{ADP}) were observed (Fig. 3D). ATP synthesis rates were proportionately reduced; thus, ATP-to-O ratios were not different (Fig. 3H).

We previously reported that mitochondrial uncoupling became evident in ob/ob and db/db mouse hearts after hearts were perfused with increased concentrations of fatty acids (5,6). Thus, palmitoyl carnitine respirations were determined in permeabilized fibers from hearts of 10-week-old Akita and control mice after perfusion with 11 mmol/l glucose and 1 mmol/l palmitate (Fig. 4A and B). Under these conditions, we observed no differences in V_{ADP}, V_{oligo}, ATP production rates, or ATP-to-O ratios. Finally, to provide more definitive evidence for the absence of mitochondrial uncoupling in Akita hearts, we isolated mitochondria from hearts of 24-week-old Akita mice after perfusion of hearts with 11 mmol/l glucose and 1 mmol/l palmitate and measured proton leak kinetics (Fig. 4C). Proton leak kinetics curves were entirely overlapping between mitochondria from Akita mice and nondiabetic controls, indicating the absence of mitochondrial uncoupling.

Expression of mitochondrial genes and mitochondrial morphology. To understand the molecular basis for impaired mitochondrial respiratory capacity with glutamate and pyruvate, we investigated gene expression in Akita and wild-type hearts at 24 weeks of age (Fig. 5A). Expression of genes encoding for subunits of the electron transport chain was reduced for four of five genes examined in Akita mice. In contrast, two forms of peroxisome proliferator–activated γ coactivator-1 (PGC-1α and PGC-1β) and their downstream mediators (nuclear respiratory factor 1 [NRF1], mitochondrial transcription factor A [TFAm], and estogen-related receptor-α [ERRα]) were not differentially expressed. Genes encoding for peroxisome proliferator–activated receptor α (PPARα) and for enzymes and transporters of fatty acid utilization did not show a uniform trend toward increased expression except

for malonyl CoA decarboxylase. Expression of GLUT1 and GLUT4 was reduced, and expression of pyruvate dehydrogenase kinase 4 (PDK4) was increased in Akita, consistent with impaired glucose oxidation in Akita. Interestingly, expression of UCP2 and UCP3 was significantly increased in Akita, and these changes were accompanied by increased expression of mitochondrial thioesterase 1 (MTE1). Consistent with increased mRNA levels, there was a twofold increase in UCP3 protein content (Fig. 5B). This observation is of particular interest because we detected no evidence of mitochondrial uncoupling in mitochondria from Akita mice.

Electron microscopy revealed markedly reduced cristae density in Akita but not in wild-type mice (Fig. 6A). Of the images evaluated, 75% showed lipid droplets in Akita mice, but no lipid droplets were observed in wild-type mice (arrows in Fig. 6A). Although mitochondrial volume density was increased in Akita mice, mitochondrial number was unchanged between the groups (Fig. 6B and C).

No evidence for oxidative stress or increased ROS in Akita hearts. Thus far, we have shown that Akita mitochondria reveal defects in oxygen consumption in the absence of mitochondrial uncoupling (despite increased UCP3 content). We previously demonstrated that in type 2 diabetic db/db mice, fatty acid–induced mitochondrial uncoupling is mediated by activation of UCPs in the presence of increased ROS production and evidence of oxidative stress. These results suggested that increased ROS is required for activation of UCPs in diabetic hearts (6). We therefore hypothesized that the absence of mitochondrial uncoupling in Akita hearts despite increased UCP3 content was due to reduced ROS in Akita hearts. Consistent with this hypothesis, there was no increase in mitochondrial H_2O_2 production. Akita mice showed a 38–46% decrease in mitochondrial H_2O_2 generation compared with wild-type mice at 10 or 24 weeks of age (Fig. 7A and D). Addition of the complex I inhibitor rotenone
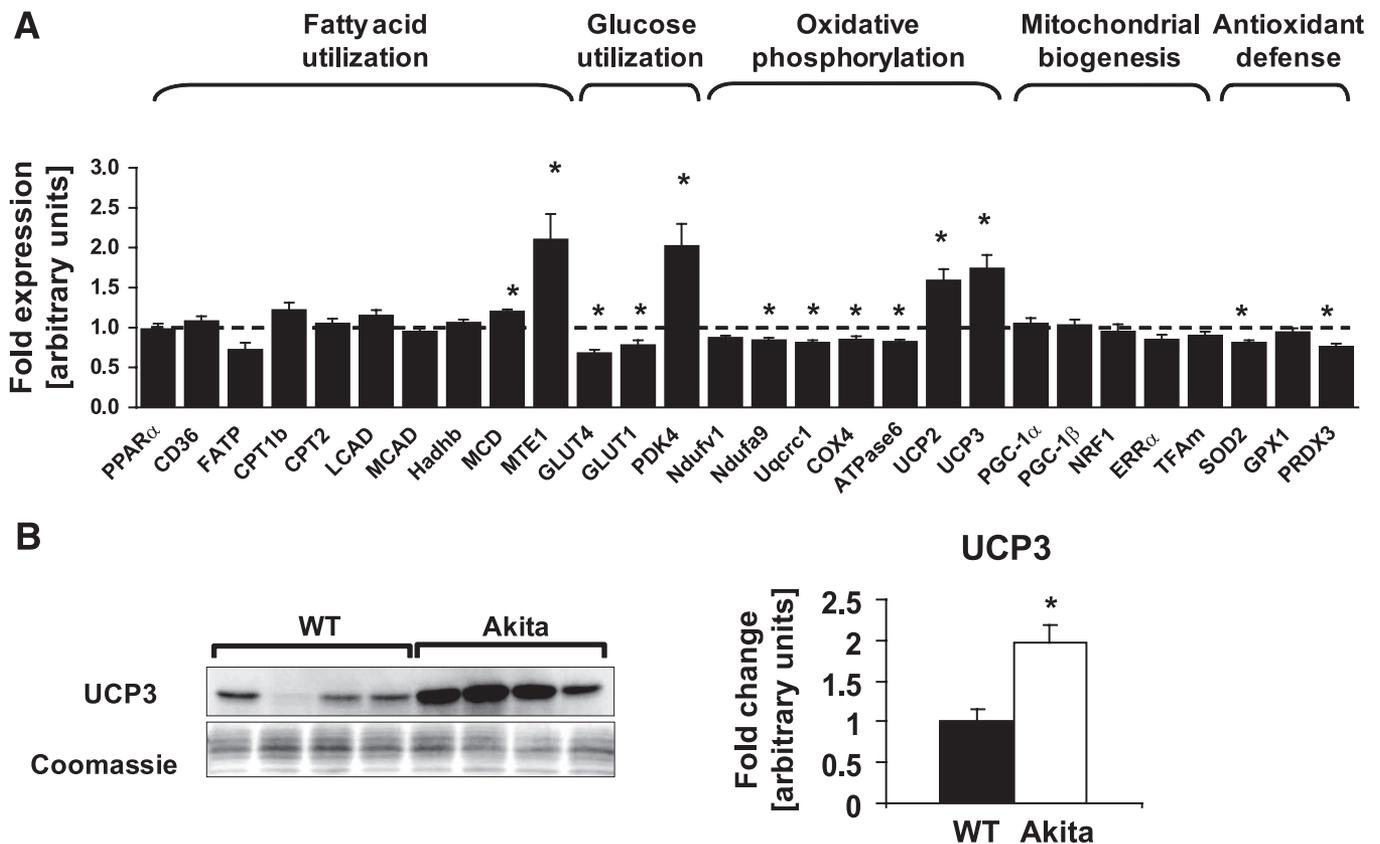
FIG. 5. Reduced OXPHOS expression and increased UCP expression. *A:* Myocardial gene expression in 24-week-old wild-type (WT) and Akita mice normalized to 16S RNA transcript levels ($n = 8$). Values represent fold change in mRNA transcript levels relative to wild type, which was assigned as one (dashed line). *B:* Representative Western blot images and densitometric quantification of UCP3 protein levels in isolated mitochondria from 24-week-old wild-type and Akita mice ($n = 4$). Coomassie blue staining was used as a loading control. *$P < 0.05$ vs. wild type.

abolished mitochondrial H_2O_2 production, suggesting that mitochondrial ROS production mainly arises from complex I in wild-type and Akita mice. Mitochondrial aconitase activity was not decreased in Akita mice at both ages (Fig. 7*B* and *E*), and oxidation of 2'-7'-dichlofluoroscein diacetate (DCFDA), a measure of tissue ROS levels, was unaltered in 24-week-old hearts (Fig. 7*C*). In addition, there was no induction of antioxidant defense pathways. Transcript levels of glutathione peroxidase 1, mitochondrial manganese superoxide dismutase (*SOD2*), and peroxiredoxin 3 (*PRDX3*) were either unchanged or even reduced in Akita (Fig. 5*A*). Similarly, protein levels of SOD2 and PRDX3 were unchanged between the groups (Fig. 7*F* and *G*).

DISCUSSION

Reduced cardiac efficiency is a well-described characteristic of type 2 diabetic hearts in animal models and humans (3,28). In this study, we addressed the following question: Do impaired cardiac efficiency and fatty acid–induced mitochondrial uncoupling contribute to cardiac contractile dysfunction in type 1 diabetic Akita mice? Similar to type 2 diabetic hearts, substrate metabolism shifts toward increased fatty acid metabolism, and mitochondrial oxidative capacity is impaired. However, in contrast to type 2 diabetic mouse models, Akita mice show relatively preserved contractile function under ambient conditions, no impairment in cardiac efficiency, and no evidence of mitochondrial uncoupling (normal V_{oligo}, ATP-to-O ratios, and proton leak). Perfusion of hearts with high fatty acid concentrations was not sufficient to induce mitochondrial uncoupling despite the presence of increased UCP3 levels. Moreover, the absence of oxidative stress distinguishes the Akita mouse from type 2 diabetic models. Thus, the molecular mechanisms for mitochondrial dysfunction importantly differ between insulin-deficient type 1 and insulin-resistant type 2 diabetic mice. We also show that increased UCP3 does not invariably lead to increased mitochondrial uncoupling in the heart, supporting the hypothesis that fatty acid–induced mitochondrial uncoupling in diabetic hearts may require a concomitant increase in ROS generation.

The absence of mitochondrial uncoupling in Akita hearts was associated with the absence of oxidative stress. Mitochondrial superoxide production, measured as H_2O_2 generation, was actually decreased, and the activity of mitochondrial aconitase and oxidation of DCFDA, which are independent measures of oxidative damage, were unaltered in Akita hearts. The association of mitochondrial uncoupling with increased ROS and lipid peroxide generation in type 2 diabetic *db/db* hearts (6) and the lack of uncoupling and the absence of oxidative stress in type 1 diabetic Akita hearts suggest a causal interdependence of ROS production and mitochondrial uncoupling in diabetic hearts. Superoxide increases proton conductance by UCP3 in isolated rat skeletal muscle mitochondria, and lipid peroxidation products, such as hydroxynonenal, increase proton leak in isolated mitochondria from multiple tissues, including the heart, via UCPs and adenine nucleotide translocator (7,24). Although fatty acids appear to be required for proton transport of UCP2 and UCP3 when reconstituted in liposomes, Echtay et al. (24) showed that

A

B
Mitochondrial volume density

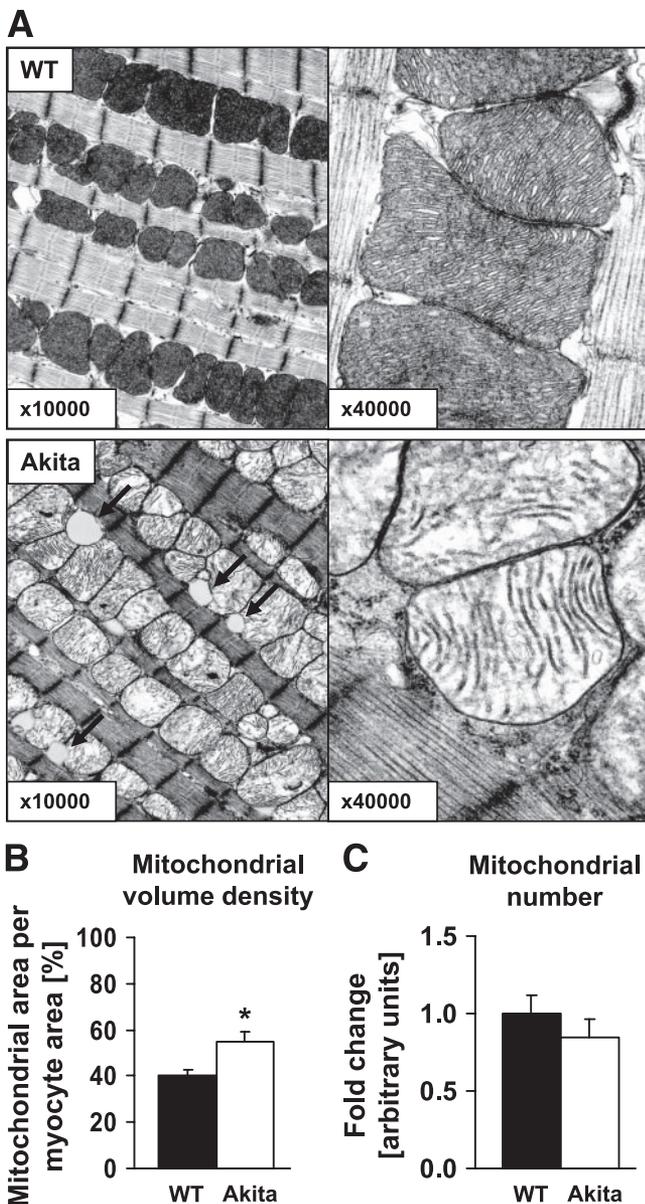## C
Mitochondrial number

FIG. 6. Altered mitochondrial morphology in Akita hearts. Representative longitudinal electron microscopy images of left ventricular wall of 24-week-old wild-type (WT) and Akita mice (A), stereological quantification of mitochondrial volume density (B), and mitochondrial number (C) (n = 4). Magnifications (×10,000 and ×40,000) are shown on each image, and black arrows on the images indicate lipid droplets. *P < 0.05 vs. wild type.

mitochondrial complex I. This was also supported by the observation that mitochondrial respirations in the presence of glutamate and pyruvate, which are complex I substrates, were also reduced, whereas this was not the case with palmitoyl carnitine that delivers reducing equivalents to complex I and complex II. Thus, a simple increase in substrate flux might not be sufficient to increase mitochondrial ROS generation in diabetic hearts in the absence of specific alterations in mitochondrial complex activities that amplify ROS generation.

Oxidative stress has been proposed to contribute to mitochondrial dysfunction in the hearts of type 1 diabetes mouse models (30,31). In the present study, we demonstrated impaired mitochondrial function and perturbed mitochondrial morphology in the absence of any evidence of oxidative stress. Interestingly, impaired mitochondrial morphology in the type 1 diabetic OVE26 mouse can be normalized by overexpression of manganese superoxide dismutase (MnSOD) or catalase in the heart, but MnSOD-deficient mice die from early dilated cardiomyopathy and have normal cardiac mitochondrial morphology (30–32). In other transgenic models, knockout of the mitochondrial transcription factor A leads to reduced mitochondrial DNA replication and transcription and enlarged mitochondria with abnormal cristae morphology, and combined deletion of the cardiac insulin and IGF1 receptor results in impaired oxidative phosphorylation (OXPHOS) gene transcription and decreased mitochondria that appeared to be less dense in electron micrographs (33–35). Thus, in some contexts, changes in the content of electron transport chain subunits can be associated with changes in mitochondrial morphology. Because insulin is a positive regulator of OXPHOS gene expression and because OXPHOS gene expression is decreased in the Akita mouse heart, insulin deficiency as opposed to oxidative stress might be an important contributor to mitochondrial dysfunction and altered morphology in the Akita mouse model (36,37). Defective insulin signaling has been reported to reduce expression levels of genes involved in β-oxidation (23), yet fatty acid oxidation genes were unchanged or increased in Akita mice. We believe that this reflects the impact of PPARα activation in the face of increased fatty acid availability.

An important observation in the present study is that increased content of UCP3 in the heart should not be taken to indicate increased mitochondrial uncoupling. We previously reported that increased mitochondrial uncoupling activity can occur in the absence of any changes in UCP3 content in hearts from *ob/ob* and *db/db* mice (5,6). It is important to discuss what might drive UCP3 levels in Akita mouse hearts. Besides detoxification of ROS, UCP3 has been postulated to play a role in the regulation of fatty acid metabolism. Conditions associated with increased fatty acid availability, such as fasting, high-fat feeding, and diabetes, result in increased UCP3 expression, likely due to increased PPARα signaling (12,38–40). In general, muscle UCP3 protein content is negatively related to fatty acid oxidative capacity, and induction of UCP3 is most pronounced in glycolytic muscle upon fasting and high-fat feeding (41,42). Thus, increased UCP3 expression may reflect an adaptive response to fatty acid overload (43). Based on the fatty acid cycling model, it has been proposed that export of fatty acid anions from the matrix into the intermembrane space via UCPs may help to lower intramitochondrial fatty acid levels if increased fatty acid availability exceeds mitochondrial oxidative

hydroxynonenal-induced proton conductance does not require the presence of fatty acids (29). Thus, it appears that for fatty acid–induced mitochondrial uncoupling, as observed to occur in type 2 diabetic hearts, an increase in ROS may be required in addition to increased fatty acid availability and utilization.

The absence of oxidative stress or of any increase in ROS or H_2O_2 production in Akita hearts was unexpected. Inhibition of mitochondrial H_2O_2 production in the presence of rotenone suggested that complex I accounted for most of the ROS production in Akita and control hearts. This contrasts with similar studies in mitochondria isolated from *db/db* hearts in which additional mitochondrial complexes (likely complex III) also contributed to ROS generation (6). The reduction in ROS generation in Akita mice suggested that there might be a defect at the level of
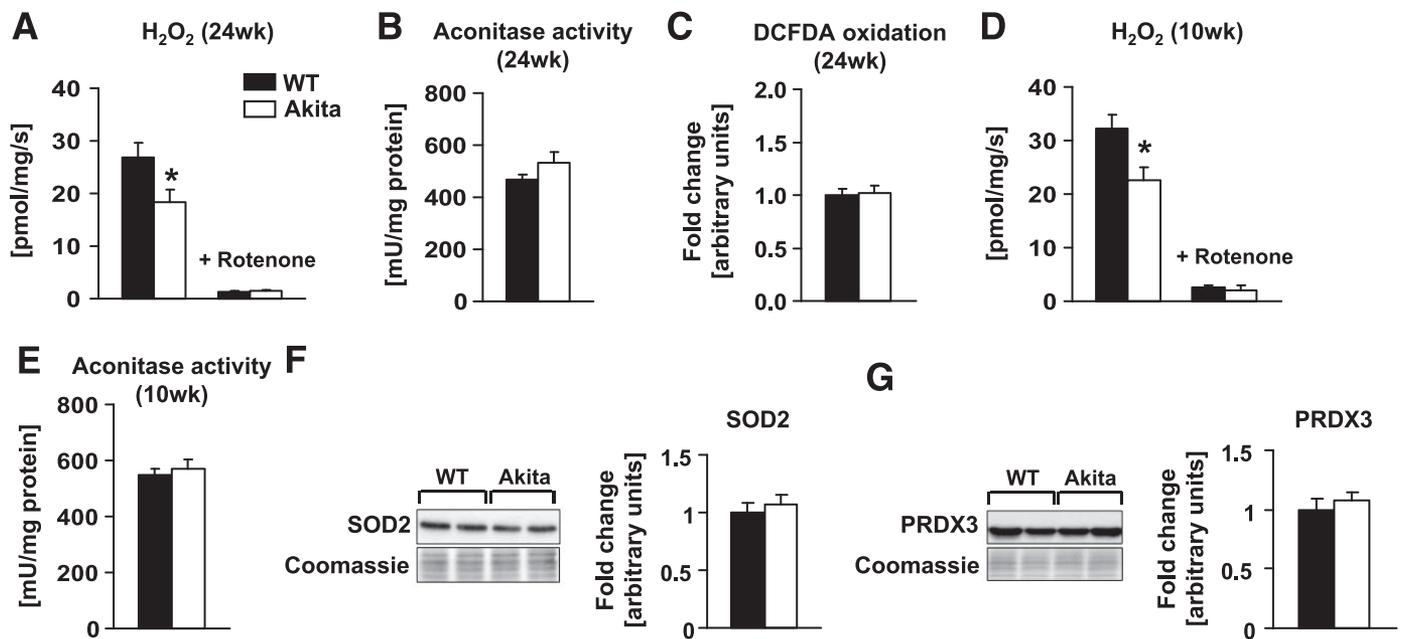
FIG. 7. Oxidative stress is absent in Akita hearts. H_2O_2 production in isolated mitochondria of wild-type (WT) and Akita mice at 24 weeks (*A*) and 10 weeks (*D*) of age ($n = 4$). Mitochondrial aconitase activity of wild-type and Akita mice at 24 weeks (*B*) and 10 weeks (*E*) of age ($n = 4$). *C*: Oxidation of DCFDA measured in cardiac whole-tissue extracts from 24-week-old wild-type and Akita mice ($n = 5$). Representative Western blot images and densitometric quantification of MnSOD (*F*) and PRDX3 (*G*) in isolated mitochondria of 24-week-old wild-type and Akita mice ($n = 4$). Coomassie blue staining was used as a loading control. *$P < 0.05$ vs. wild type.

capacity (43–45). Thereby, oxidation of intramitochondrial fatty acids into harmful lipid peroxides could be prevented. Expression of MTE1 often parallels that of UCP3, and this was also the case in the present study. MTE1 catalyzes conversion of acyl-CoAs back to fatty acid anions, which can then be translocated out of the matrix by UCPs (13,29). In the cytosol, they may be reesterified and oxidized in the mitochondria, stored as triglycerides, or used for other pathways. Nonesterified fatty acids can be generated within mitochondria and exported from the matrix, and these events are markedly increased in cardiac mitochondria from streptozotocin-induced type 1 diabetic rats (13). Despite increased basal fatty acid oxidation, Akita mice also revealed increased lipid droplets; thus, it is tempting to speculate that fatty acyl-CoAs would be converted to fatty acid anions by increased MTE1 activity, exported by UCP3, reesterified, and stored as triglycerides. Thus, UCPs would contribute to match fatty acid availability with oxidation to prevent intramitochondrial lipotoxic effects.

A number of important differences between Akita mice and previously evaluated models of type 2 diabetes were observed (3–6,8). First, there was a relative preservation of cardiac function and preserved inotropic responses to a calcium-induced increase in workload. This likely reflects the more profound mitochondrial dysfunction in the type 2 models and a greater degree of mitochondrial uncoupling. Preliminary studies do suggest, though, that cardiac dysfunction may develop in Akita mice after a longer-term hemodynamic challenge, such as after isoproterenol infusion (supplementary results and supplementary Table 5), but the mechanisms for this remains to be elucidated. Second, insulin sensitivity was preserved in Akita hearts in contrast to the insulin resistance reported in models of type 2 diabetes (2,3). Although insulin levels in diabetic Akita are 40% of insulin levels in nondiabetic controls (19), these ambient insulin concentrations might be sufficient to

maintain mitochondrial function to a greater extent than models in which insulin signaling is severely impaired. Finally, myocardial V_{O_2} was not increased despite increased oxidation rates of exogenous palmitate. Although this may partly reflect the absence of mitochondrial uncoupling, it is also possible that reduced oxidation of glucose and endogenous triglycerides coupled with mitochondrial dysfunction reduced myocardial V_{O_2} in intact perfused hearts.

In conclusion, despite a significant increase in UCP3 content, insulin-deficient Akita hearts do not develop fatty acid–induced mitochondrial uncoupling, suggesting that underlying mechanisms for mitochondrial dysfunction may importantly differ between insulin-responsive type 1 versus insulin-resistant type 2 diabetic hearts. Increased UCP3 levels do not invariably lead to increased mitochondrial uncoupling in the heart, thereby supporting the hypothesis that fatty acid–induced mitochondrial uncoupling in diabetic hearts requires a concomitant increase in ROS or lipid peroxide generation.

REFERENCES

1. Boudina S, Abel ED: Mitochondrial uncoupling: a key contributor to reduced cardiac efficiency in diabetes. *Physiology* 21:250–258, 2006
2. Bugger H, Abel ED: Molecular mechanisms for myocardial mitochondrial dysfunction in the metabolic syndrome. *Clin Sci* 114:195–210, 2008

3. Mazumder PK, O'Neill BT, Roberts MW, Buchanan J, Yun UJ, Cooksey RC, Boudina S, Abel ED: Impaired cardiac efficiency and increased fatty acid oxidation in insulin-resistant *ob/ob* mouse hearts. *Diabetes* 53:2366–2374, 2004

4. Buchanan J, Mazumder PK, Hu P, Chakrabarti G, Roberts MW, Yun UJ, Cooksey RC, Litwin SE, Abel ED: Reduced cardiac efficiency and altered substrate metabolism precedes the onset of hyperglycemia and contractile dysfunction in two mouse models of insulin resistance and obesity. *Endocrinology* 146:5341–5349, 2005

5. Boudina S, Sena S, O'Neill BT, Tathireddy P, Young ME, Abel ED: Reduced mitochondrial oxidative capacity and increased mitochondrial uncoupling impair myocardial energetics in obesity. *Circulation* 112:2686–2695, 2005

6. Boudina S, Sena S, Theobald H, Sheng X, Wright JJ, Hu XX, Aziz S, Johnson JI, Bugger H, Zaha VG, Abel ED: Mitochondrial energetics in the heart in obesity-related diabetes: direct evidence for increased uncoupled respiration and activation of uncoupling proteins. *Diabetes* 56:2457–2466, 2007

7. Echtay KS, Roussel D, St-Pierre J, Jekabsons MB, Cadenas S, Stuart JA, Harper JA, Roebuck SJ, Morrison A, Pickering S, Clapham JC, Brand MD: Superoxide activates mitochondrial uncoupling proteins. *Nature* 415:96–99, 2002

8. How OJ, Aasum E, Severson DL, Chan WY, Essop MF, Larsen TS: Increased myocardial oxygen consumption reduces cardiac efficiency in diabetic mice. *Diabetes* 55:466–473, 2006

9. Flarsheim CE, Grupp IL, Matlib MA: Mitochondrial dysfunction accompanies diastolic dysfunction in diabetic rat heart. *Am J Physiol* 271:H192–H202, 1996

10. Tahiliani AG, Lopaschuk GD, McNeill JH: Effect of insulin treatment on long-term diabetes-induced alteration of myocardial function. *Gen Pharmacol* 15:545–547, 1984

11. Turko IV, Li L, Aulak KS, Stuehr DJ, Chang JY, Murad F: Protein tyrosine nitration in the mitochondria from diabetic mouse heart: implications to dysfunctional mitochondria in diabetes. *J Biol Chem* 278:33972–33977, 2003

12. Murray AJ, Panagia M, Hauton D, Gibbons GF, Clarke K: Plasma free fatty acids and peroxisome proliferator-activated receptor α in the control of myocardial uncoupling protein levels. *Diabetes* 54:3496–3502, 2005

13. Gerber LK, Aronow BJ, Matlib MA: Activation of a novel long-chain free fatty acid generation and export system in mitochondria of diabetic rat hearts. *Am J Physiol Cell Physiol* 291:C1198–C1207, 2006

14. Lashin O, Romani A: Mitochondria respiration and susceptibility to ischemia-reperfusion injury in diabetic hearts. *Arch Biochem Biophys* 420:298–304, 2003

15. King KL, Young ME, Kerner J, Huang H, O'Shea KM, Alexson SE, Hoppel CL, Stanley WC: Diabetes or peroxisome proliferator-activated receptor alpha agonist increases mitochondrial thioesterase I activity in heart. *J Lipid Res* 48:1511–1517, 2007

16. Bolzan AD, Bianchi MS: Genotoxicity of streptozotocin. *Mutat Res* 512:121–134, 2002

17. Lashin O, Romani A: Hyperglycemia does not alter state 3 respiration in cardiac mitochondria from type-I diabetic rats. *Mol Cell Biochem* 267:31–37, 2004

18. Hsueh W, Abel ED, Breslow JL, Maeda N, Davis RC, Fisher EA, Dansky H, McClain DA, McIndoe R, Wassef MK, Rabadan-Diehl C, Goldberg IJ: Recipes for creating animal models of diabetic cardiovascular disease. *Circ Res* 100:1415–1427, 2007

19. Yoshioka M, Kayo T, Ikeda T, Koizumi A: A novel locus, Mody4, distal to D7Mit189 on chromosome 7 determines early-onset NIDDM in nonobese C57BL/6 (Akita) mutant mice. *Diabetes* 46:887–894, 1997

20. Ron D: Proteotoxicity in the endoplasmic reticulum: lessons from the Akita diabetic mouse. *J Clin Invest* 109:443–445, 2002

21. Barber AJ, Antonetti DA, Kern TS, Reiter CE, Soans RS, Krady JK, Levison SW, Gardner TW, Bronson SK: The Ins2Akita mouse as a model of early retinal complications in diabetes. *Invest Ophthalmol Vis Sci* 46:2210–2218, 2005

22. Gurley SB, Clare SE, Snow KP, Hu A, Meyer TW, Coffman TM: Impact of genetic background on nephropathy in diabetic mice. *Am J Physiol Renal Physiol* 290:F214–F222, 2006

23. Belke DD, Betuing S, Tuttle MJ, Graveleau C, Young ME, Pham M, Zhang D, Cooksey RC, McClain DA, Litwin SE, Taegtmeyer H, Severson D, Kahn CR, Abel ED: Insulin signaling coordinately regulates cardiac size, metabolism, and contractile protein isoform expression. *J Clin Invest* 109:629–639, 2002

24. Echtay KS, Esteves TC, Pakay JL, Jekabsons MB, Lambert AJ, Portero-Otin M, Pamplona R, Vidal-Puig AJ, Wang S, Roebuck SJ, Brand MD: A signalling role for 4-hydroxy-2-nonenal in regulation of mitochondrial uncoupling. *EMBO J* 22:4103–4110, 2003

25. Weibel E: Steriological principles for morphometry in electron microscopic cytology. *Int Rev Cytol* 26:235–302, 1979

26. Kim HJ, Kim KW, Yu BP, Chung HY: The effect of age on cyclooxygenase-2 gene expression: NF-kappaB activation and IkappaBalpha degradation. *Free Radic Biol Med* 28:683–692, 2000

27. Yan LJ, Levine RL, Sohal RS: Oxidative damage during aging targets mitochondrial aconitase. *Proc Natl Acad Sci U S A* 94:11168–11172, 1997

28. Peterson LR, Herrero P, Schechtman KB, Racette SB, Waggoner AD, Kisrieva-Ware Z, Dence C, Klein S, Marsala J, Meyer T, Gropler RJ: Effect of obesity and insulin resistance on myocardial substrate metabolism and efficiency in young women. *Circulation* 109:2191–2196, 2004

29. Jaburek M, Varecha M, Gimeno RE, Dembski M, Jezek P, Zhang M, Burn P, Tartaglia LA, Garlid KD: Transport function and regulation of mitochondrial uncoupling proteins 2 and 3. *J Biol Chem* 274:26003–26007, 1999

30. Ye G, Metreveli NS, Donthi RV, Xia S, Xu M, Carlson EC, Epstein PN: Catalase protects cardiomyocyte function in models of type 1 and type 2 diabetes. *Diabetes* 53:1336–1343, 2004

31. Shen X, Zheng S, Metreveli NS, Epstein PN: Protection of cardiac mitochondria by overexpression of MnSOD reduces diabetic cardiomyopathy. *Diabetes* 55:798–805, 2006

32. Li Y, Huang TT, Carlson EJ, Melov S, Ursell PC, Olson JL, Noble LJ, Yoshimura MP, Berger C, Chan PH, Wallace DC, Epstein CJ: Dilated cardiomyopathy and neonatal lethality in mutant mice lacking manganese superoxide dismutase. *Nat Genet* 11:376–381, 1995

33. Wang J, Wilhelmsson H, Graff C, Li H, Oldfors A, Rustin P, Bruning JC, Kahn CR, Clayton DA, Barsh GS, Thoren P, Larsson NG: Dilated cardiomyopathy and atrioventricular conduction blocks induced by heart-specific inactivation of mitochondrial DNA gene expression. *Nat Genet* 21:133–137, 1999

34. Larsson NG, Wang J, Wilhelmsson H, Oldfors A, Rustin P, Lewandoski M, Barsh GS, Clayton DA: Mitochondrial transcription factor A is necessary for mtDNA maintenance and embryogenesis in mice. *Nat Genet* 18:231–236, 1998

35. Laustsen PG, Russell SJ, Cui L, Entingh-Pearsall A, Holzenberger M, Liao R, Kahn CR: Essential role of insulin and insulin-like growth factor 1 receptor signaling in cardiac development and function. *Mol Cell Biol* 27:1649–1664, 2007

36. Huang X, Eriksson KF, Vaag A, Lehtovirta M, Hansson M, Laurila E, Kanninen T, Olesen BT, Kurucz I, Koranyi L, Groop L: Insulin-regulated mitochondrial gene expression is associated with glucose flux in human skeletal muscle. *Diabetes* 48:1508–1514, 1999

37. Stump CS, Short KR, Bigelow ML, Schimke JM, Nair KS: Effect of insulin on human skeletal muscle mitochondrial ATP production, protein synthesis, and mRNA transcripts. *Proc Natl Acad Sci U S A* 100:7996–8001, 2003

38. Tunstall RJ, Mehan KA, Hargreaves M, Spriet LL, Cameron-Smith D: Fasting activates the gene expression of UCP3 independent of genes necessary for lipid transport and oxidation in skeletal muscle. *Biochem Biophys Res Commun* 294:301–308, 2002

39. Weigle DS, Selfridge LE, Schwartz MW, Seeley RJ, Cummings DE, Havel PJ, Kuijper JL, BeltrandelRio H: Elevated free fatty acids induce uncoupling protein 3 expression in muscle: a potential explanation for the effect of fasting. *Diabetes* 47:298–302, 1998

40. Young ME, Patil S, Ying J, Depre C, Ahuja HS, Shipley GL, Stepkowski SM, Davies PJ, Taegtmeyer H: Uncoupling protein 3 transcription is regulated by peroxisome proliferator-activated receptor (alpha) in the adult rodent heart. *FASEB J* 15:833–845, 2001

41. Hoeks J, Hesselink MK, van Bilsen M, Schaart G, van der Vusse GJ, Saris WH, Schrauwen P: Differential response of UCP3 to medium versus long chain triacylglycerols: manifestation of a functional adaptation. *FEBS Lett* 555:631–637, 2003

42. Schrauwen P, Hoppeler H, Billeter R, Bakker AH, Pendergast DR: Fiber type dependent upregulation of human skeletal muscle UCP2 and UCP3 mRNA expression by high-fat diet. *Int J Obes Relat Metab Disord* 25:449–456, 2001

43. Schrauwen P, Hoeks J, Hesselink MK: Putative function and physiological relevance of the mitochondrial uncoupling protein-3: involvement in fatty acid metabolism? *Prog Lipid Res* 45:17–41, 2006

44. Garlid KD, Jaburek M, Jezek P: The mechanism of proton transport mediated by mitochondrial uncoupling proteins. *FEBS Lett* 438:10–14, 1998

45. Himms-Hagen J, Harper ME: Physiological role of UCP3 may be export of fatty acids from mitochondria when fatty acid oxidation predominates: an hypothesis. *Exp Biol Med* (*Maywood*) 226:78–84, 2001